# Real-time monitoring of atmospheric ammonia during a pollution episode in Madrid (Spain)

Begoña Artíñano, Manuel Pujadas, Elisabeth Alonso-Blanco, Marta Becerril-Valle, Esther Coz, Francisco J. Gómez-Moreno, Pedro Salvador, Lourdes Nuñez, Magdalena Palacios, Elías Diaz

CIEMAT, Environment Department, Av. Complutense 40, E-28040 Madrid, Spain

## 1. Introducción

Atmospheric ammonia ($NH_3$) is an alkaline gas that is present in the atmosphere where it plays a significant role as neutralizing agent of acidic species, forming particle-phase ammonium ($NH_4^+$) salts. $NH_3$ preferentially reacts with sulfuric acid ($H_2SO_4$) to form stable ammonium sulfate ($(NH_4)_2SO_4$) and/or ammonium bisulfate ($NH_4HSO_4$) (Harrison and Jones, 1995). When excess $NH_3$ is available it combines with nitric acid or chloric acid to generate ammonium nitrate ($NH_4NO_3$) and ammonium chloride ($NH_4Cl$), respectively. These species present a reversible equilibrium (Seinfeld and Pandis, 2016) depending on temperature and relative humidity conditions in the atmosphere. These chemical reactions are probably the most important for secondary aerosol formation, being highly dependent on $NH_3$, $NO_x$ and $SO_x$ concentrations and thermodynamic variables. In addition to this dominant role in the formation of secondary atmospheric species influencing air quality, ammonia is an important source of soil nutrients but can pose an important threat for ecosystems and global nitrogen cycle due to its acidifying and eutrophying effects (Van Breemen et al., 1982; Bobbink et al., 2010). Finally, it can cause direct adverse effects on human health due to overexposure (Ryder–Powder, 1991).

Although ammonia can be found naturally in the atmosphere, anthropogenic activities such as cattle and agriculture present the main sources of emissions. The most important sources are livestock waste and the use of nitrogen fertilizers, respectively, which additionally generate high nitrate concentration in surface waters. In the European inventories, agriculture is considered to be the main sector for ammonia emissions, accounting for 90% of the total emissions (EEA, 2013). The remaining 10% of the total emissions is allocated to other anthropogenic sources, such as some industrial activities (textile plastics, explosives, pulp and paper, food and drinking, domestic cleaning products, refrigerants, etc.), road transport, waste generation and treatment, and other diffuse sources (Sutton et al., 2000; Perrino et al., 2002; Reche et al., 2015).

Consequently, in global terms the highest ambient ammonia concentrations are recorded in rural continental areas, particularly if little $SO_4^{2-}$ is present, although this distribution can be modulated at the local scale by specific geographical features (Pay et al., 2012). Local emission sources and climatology

condition the gas phase prevalence of $NO_3^-$ in some regions (Perrino et al., 2002), as low temperatures and high relative humidity shift the ammonia equilibrium to the aerosol phase (Trebs et al., 2004). In general terms, it is noteworthy that higher levels of ammonia are expected in summer, whereas other thermodynamic variables such as relative humidity can contribute to stabilizing $NH_4NO_3$ even during mild summer temperatures. The seasonal pattern is more evident in rural sites, where agricultural and husbandry practices (fertilizer application, storage and treatment of manure) and soil characteristics modulate the ambient ammonia variability. This seasonal variation has also been documented in some urban areas, despite the great spatial variability of ammonia concentrations that can be mostly attributed to the direct influence of local sources (Perrino et al., 2002; Phan et al., 2013; Reche et al., 2012, 2015). Additionally, air masses that have originated or passed over ammonia-rich zones, e.g. rural or industrial sites, in specific situations can contribute to increasing the observed $NH_3$ concentrations inside the urban areas (Wang et al., 2015).

Road traffic has been recognized as a source of urban $NH_3$ (Sutton et al., 2000; Perrino et al., 2002; Battye et al., 2003; Heeb et al., 2008; Reche et al., 2012; Sun et al., 2016; Chang et al., 2016). Three-way catalytic converters in petrol engines and selective catalytic reduction by addition of urea in diesel vehicles have become important sources of reduced nitrogen compounds, contributing to the urban atmospheres with an additional input of $NH_3$ emissions (Nowak et al., 2012). Catalyst temperatures and air-to-fuel ratios have been found to be the key parameters determining the extent of $NH_3$ formation and enhancing the ammonia production in cities (Phan et al., 2013; Link et al., 2017). Nevertheless, in terms of ammonia emissions, it is difficult to estimate the road traffic source, which is usually omitted in most of these emissions inventories (EEA, 2013) that are largely focused on the main sources, such as agriculture and cattle and to a lesser extent to some industrial activities. Although the European legislation (National Emission Ceilings Directive, 2016/2284/EU) contemplates ammonia among the list of pollutants for national emissions reporting from member states, setting important reduction commitments, at present there are no quality objectives for ambient concentrations of this pollutant. Nevertheless, in 2011 the Spanish legislation (Royal Decree R.D. 102/2011) considered the necessity of measuring ambient air ammonia and imposed its monitoring, regarding background sources at both regional and rural levels, and at urban traffic stations in the main urban nuclei (> 500,000 inhabitants).

It should be noted that action plans that are aimed to reduce secondary air pollutants are currently based on the control of precursor gaseous emissions from regulated anthropogenic sources. The decline in $NH_3$ emissions in recent decades in Europe has been very slow due to the high uncertainties associated with ammonia emissions and sources. This has been postulated to be the reason why strong reductions in $SO_2$ and $NO_x$ emissions have produced less than expected abatements in sulfate and nitrate concentrations

(Salvador, 2018, and references therein). Moreover, reductions in $SO_2$ can lead to increases in nitrate concentrations (Harrison et al., 2013), possibly due to the greater availability of ammonia to influence the ammonium nitrate dissociation equilibrium. Hence, the uncertainties associated with ammonia emissions, together with the huge nonlinearities in the relationship between precursor emissions and ambient concentrations of secondary particulate matter (PM), are causing difficulties in abating particulate ammonium sulfate and nitrate levels which have a large influence on $PM_{2.5}$ concentrations.

Ammonia concentrations in urban areas have been widely studied by mostly using passive sampling techniques (Perrino et al., 2002; Reche et al., 2012, 2015; Meng et al., 2011; Chang et al., 2016) although other off-line techniques such as annular denuders have also been used (Biswas et al., 2008; Ianniello et al., 2010; Upadhyay et al., 2013). The low time resolution of ammonia concentrations in these studies (averaging time scales between 7 and 30 days) is generally linked to the field campaign duration and conditioned by the sampling and the analysis techniques. However, short term variations of $NH_3$ can become significant when taking into account the life-time of this gas in the atmosphere (less than 5 days) (Warneck, 2000) and the variability of ammonia sources (Perrino et al., 2002; Pandolfi et al., 2012; Phan et al., 2013; Reche et al., 2012; Revuelta et al., 2012).

Although some off-line methods can be very valuable scientifically and cost-effective for mapping ammonia concentration based on high number of measurement points, they lack sufficient time resolution with which to interpret short-term variations. This feature is relevant in identifying specific local sources or deepening the knowledge of the atmospheric processes that lead to the formation of secondary particulates.

There is a wide range of techniques for monitoring inorganic species including ammonia, such as Wavelength-Scanned Cavity Ring Down Spectroscopy (WS-CRDS), External-Cavity Quantum Cascade Laser (ECQCL), Inorganic Continuous Aerosol Measurement System (iCAMS), Chemical Ionization Mass Spectrometer (CIMS), Differential Optical Absorption Spectroscopy (DOAS), or Monitor for AeRosols and GAses (MARGA) multipollutant instrument (Wang et al., 2015, and references therein; You et al., 2014). Some of these techniques have recently been introduced in the field of atmospheric science and their ability to measure these species in real-time has proved that they are useful tools for these purposes.

One such technique, Cavity-Enhanced Laser Absorption Spectroscopy (CELAS), has been used in the present study for undertaking continuous measurements of ambient ammonia during a field campaign that was carried out in Madrid (Spain) and which coincided with a winter pollution episode.

In previous documented studies (Revuelta et al., 2014; Reche et al., 2015) that were based in Madrid, ambient ammonia concentrations were measured using passive sampling, whereas to our knowledge

there are no previous studies that were based on other techniques. The objective of this study was to characterize the short-term variations of $NH_3$ and their relationship with emissions from specific urban sources. The influence of a wastewater treatment plant affecting the observed concentrations has been assessed. Additionally, their impact on the aerosol composition and other physico-chemical properties at an urban background site has also been analyzed. Measurements of some aerosol properties such as size-segregated distributions of particle number and chemical composition have provided some insights into the formation processes of secondary aerosol.

## 2. Methodology

### *2.1. Experimental site and measurement period*

Measurements were performed on the second floor (of height 4 m) of a building at the CIEMAT facilities in Madrid, Spain (40° 27′ 23.2″ N, 03° 43′ 32.3″ W). The CIEMAT facilities are located in a non-residential area at the edge of the main University Campus approximately 8 km north-west of the city center (Fig. 1), hence, the experimental site is representative of the urban background. The main atmospheric pollution sources in city of Madrid are road transport and residential, commercial and institutional sectors, mainly through heating devices in the cold season. There are no significant heavy industrial activities influencing the air quality of the city (Ayuntamiento de Madrid, 2016). The population living within the metropolitan area reaches approximately 6 million inhabitants, which implies a car fleet of almost 4.5 million vehicles (2465 car $km^{-2}$, 53% being diesel vehicles) circulating by the main radial highways and ring roads surrounding the city (https:// sedeapl.dgt.gob.es/IEST2/). The main traffic routes that eventually influence the measurement site of this study are the A6 radial highway connecting the city of Madrid with the North-Western sector of Spain, and several avenues and streets of the university, district with low to moderate traffic intensity, where the experimental site is located.

From a climate perspective, Madrid has a continental Mediterranean climate with extreme temperatures in summer and winter. The warmest months are July and August that record the maximum monthly averages (24.5 °C, climatological average value). This means that daily maxima of 40 °C are not infrequent in the summer months, and this value was frequently surpassed in the last five years, which have experienced severe heat waves. The summer period is also the driest period, characterized by a mean relative humidity (RH) < 40% and mean rainfall values < 10–15 mm. The coldest months are January and December (6–8 °C monthly mean temperature) whereas RH (77–79%) reaches its annual maxima during these months.

In fall and winter seasons, the Madrid area frequently experiences episodes of strong atmospheric stability, mainly associated to the presence of subsidence anticyclones that favor the accumulation of pollutants, thereby increasing the ambient pollutant concentrations at the surface level. The ammonia measurements that were analyzed in the present study were carried out from 1December15, 2014 to January13, 2015, coinciding with one of these strong stability episodes. Ambient temperatures ranging from −2 °C to 14 °C (hourly values), typical of winter weather, were recorded during the experimental period. Additionally, some of the measurement days coincided with Christmas time and the end of the year, which are two special periods when traffic patterns and population habits are somewhat different from those that are typical of other winter days.

### *2.2. Measurements and data analysis*

Ammonia measurements were performed using a portable instrument (LGR Model 914–1012 $NH_3/H_2O$) based on the CELAS technique (Romanini et al., 2014). The instrument used in the present study is an enhanced performance version with fast flow capability and including enhanced thermal stability to provide ultra-stable measurements of $NH_3$. High conductance plumbing in this instrument allows 1–100 Hz flow response and measurement of the continuous spectra avoids interferences with other species, hence the measurement has an autoselective focus. Time resolution during the measurement period was approximately 1 min.

Simultaneous measurements of other atmospheric pollutants were performed at the same site during the experimental study. Gaseous species ($SO_2$, NO, $NO_2$, and $O_3$) were obtained by using a DOAS spectrometer (OPSIS-AR-500) with a 10-min resolution and a measurement optical path of 228 m. Ambient aerosol mass concentrations (10-min resolution) were monitored by an optical particle counter instrument (GRIMM 1107) that was calibrated against reference gravimetric measurements for the $PM_{10}$, $PM_{2.5}$ and $PM_1$ size fractions at the same experimental site. Particle number size distributions (PNSDs) were obtained by using a Scanning Mobility Particle Sizer (SMPS) consisting of a Differential Mobility Analyzer (TSI-SMPS: DMA 3081) connected to a Condensation Particle Counter (CPC; TSI Model 3775). This instrument provided measurements of duration 4.5 min into 107 channels (14.6–661.2 nm) of the submicron aerosol fraction.

Aerosol chemical composition was provided by an Aerosol Chemical Speciation Monitor (ACSM, Aerodyne Research Inc., MA, USA) that measured the non-refractory submicron concentration components (i.e. organic matter, nitrate, sulfate, ammonium and chloride) of the ambient aerosol with a time resolution of around 30 min. The SMPS and ACSM instruments are included in the Aerosol Clouds and Trace Gases Research InfraStructure (ACTRIS) (http://www.actris.eu/) the European network aimed at improving and harmonizing observations of the in-situ aerosol properties. Measurement and quality control protocols of

ACTRIS including international intercomparison exercises (Crenn et al., 2015) were applied to these two instruments. The SMPS also participated in some national intercomparison exercises through the Spanish Network of Environmental DMAs (REDMAAS) (GómezMoreno et al., 2015). These data were used to interpret the formation of secondary inorganic aerosol, mainly ammonium nitrate in the present study.

Meteorological variables of ambient temperature at 3 m a.g.l (lower temperature LT) and 54 m a.g.l. (upper temperature UT), precipitation and solar irradiance at 34 m a.g.l., relative humidity at 3 m a.g.l., and wind speed and direction at 54 m a.g.l. were recorded with a frequency of 10 minat the weather station operating at the CIEMAT site. This station is calibrated twice per year following the requirements and standards of the Spanish Regulatory Nuclear Safety Council (CSN).

The OPENAIR package R (Carslaw and Ropkins, 2012), (R Development, http://www.openair-project.org/) was used for the analysis and interpretation of measurements. Polar plot diagrams were constructed for different pollutants using wind speed and direction data. A resolution of 10 min was used whenever possible.

Ancillary hourly data on gaseous pollutants (NO, $NO_2$ and CO) and particle matter ($PM_{10}$ and $PM_{2.5}$) from the monitoring stations of the municipality-based Madrid air quality monitoring network (AQMN) were eventually used to support data interpretation.

## 3. Results and discussion

### *3.1. Meteorological analysis*

Meteorological conditions were characterized at the synoptic scale by the presence of a persistent strong anticyclone (1030 hPa mean sea level pressure) located over the Azores Islands (situated in mid-Atlantic Ocean, 1564 km west of Portugal). This situation affected the whole Iberian Peninsula during most of the measurement period. Only three short ventilation events occurred during the periods of December 21–23 and December 28–30, 2014 and January 11–12, 2015 when moderate (> 8 m $s^{-1}$) to strong (> 12 m $s^{-1}$) north-easterly and northern winds blew over the Madrid area due to northward displacements of the highpressure center. The rest of the days of the experimental period experienced conditions of calm winds (wind speed < 2 m $s^{-1}$) and clear skies. On these days of strong atmospheric stability and high diurnal thermal amplitude, ambient temperature followed a marked diurnal cycle, ranging between −2.5 °C and 15.6 °C, minimum and maximum daily values recorded, respectively (Table S1). Thus, the point of influence of the temperature on ammonium nitrate gas phase partitioning by volatilization (Seinfeld and Pandis, 2016) was never reached, favoring the aerosol phase of this species. Relative humidity was rather variable, ranging from 10.5 to 95.8% during the measurement period. Calm wind conditions (2.1 m $s^{-1}$ average

hourly value) enhanced the formation of surface thermal inversions during a great part of the period. These were, in summary, the most characteristic meteorological features during the experimental phase.

During the first week of January 2015 the high-pressure system became deeper, increasing the surface layer stability that triggered an over-accumulation of air pollutants in the whole of the Madrid airshed. Except for the short windy periods, a general increase of ambient concentrations for all pollutants was observed in the Madrid AQMN stations (Fig. S1). In general, time series exhibited a progressive increase of pollutant concentrations that remained high until January 13, 2015 coinciding with the end of the episode. This was linked to the pass of a frontal system accompanied by precipitations on January 15, 2015 that cleaned up the atmosphere.

### *3.2. Ammonia concentrations and relationships with road traffic and meteorology*

Mean ammonia concentration recorded during the measurement period was 2.2 ± 1.7 $\mu gm^{-3}$ with a 10-min maximum of 9.3 $\mu gm^{-3}$ recorded on January 13, 2015 at 17:00 h local time (LT). This mean value is similar to the value obtained at the same experimental site for Autumn–Winter in a previous study using passive sampling techniques (Revuelta et al., 2014). It is also in the range of values (1.5–3.9 $\mu g\ m^{-3}$) obtained at urban background sites in Spain, although it exceeds the average value obtained in urban background sites in Madrid (1.5 ± 0.3–1.6 ± 0.3 $\mu g\ m^{-3}$) (Revuelta et al., 2014; Reche et al., 2015). In the present work, it was assumed that meteorological conditions could have played an important role in the observed concentrations. Although high pollutant concentrations were recorded in the first part of the episode, the highest absolute concentrations were recorded during the second part, from December 30, 2014 to January 13, 2015, once the frontal system swept over and cleaned up the area on December 28, 2014 (Fig. S1). Since that day, a progressive increase of daily maxima and mainly nocturnal minima led to the critical part of the pollution episode.

In this period, ammonia concentrations exhibited an increase during the afternoon with two marked maxima on some days (Fig. 2). Other pollutants such as gaseous species (NO, $NO_2$, $SO_2$) and particulate matter did not present a clear pattern of evolution. Particulate nitrate seemed to evolve in a similar way, although no statistical relationship has been found and their maxima precede those of $NH_3$. This is due to the fact that while there is an availability of nitric acid, ammonium nitrate is formed and reaches the site, whereas when ammonium nitrate is reduced it is the ammonia that is transported.

In general terms, no statistically significant linear relationships have been found between $NH_3$ and other air pollutants or meteorological parameters such as temperature and relative humidity (Table S2). Nevertheless, as some of these pollutants such as $SO_2$ or $NO_2$ react with $NH_3$ as part of the secondary

aerosol formation processes, relationships between secondary inorganic compounds formed from these precursor gases have been investigated in terms of equivalents.

It is noteworthy that the behavior of the pollutant series during the first day of 2015, which recorded relatively high nocturnal values of $NO_x$ and daily maxima of particles at the experimental site, also showed in the average for all the AQMN stations (Fig. S1). This fact, which can be attributed to the nocturnal traffic and anthropogenic activity of that day, did not appear to have any influence on the ambient levels of ammonia that were measured at the experimental site. Ammonia concentrations showed a well-defined pattern exhibiting two daily maxima centered approximately at 17:00 h (LT) during the last four days of the episode. An early morning relative increase was also observed on some specific days.

These results provide evidence that despite the relationships of ambient ammonia concentrations with traffic-related pollutants, such as CO and $NO_2$, found by other researchers at urban sites, the ammoniatraffic relation cannot be extrapolated for all sites and situations and it is not so clear in terms of short-term variations. This conclusion is in line with results obtained in previous studies for other urban areas such as Rome in Italy (Perrino et al., 2002), Seoul in South Korea (Phan et al., 2013) and Barcelona in Spain (Pandolfi et al., 2012) where the correlation with traffic-related pollutants is high at the traffic sites, medium at the residential sites, and low at the urban background sites such as the one in the present study.

However, it can be seen in Fig. 2 that the ammonia daily maximum seems to match approximately the ambient temperature maximum. In fact, both series presented a similar time evolution, suggesting that ambient ammonia concentrations could be partially modulated by this meteorological variable. An ammonia-temperature relationship was suggested by Perrino et al. (2002) based on seasonal measurement campaigns carried out in Rome. Phan et al. (2013) found significant determination coefficients for linear correlations between $NH_3$ and air temperature at two urban sites in Seoul, mainly for winter periods, whereas You et al. (2014) obtained an association between both parameters in the range of 17–22 °C through an exponential fitting in the Southeastern Aerosol Research and Characterization (SEARCH) Centreville, AL, USA. A similar dependence approaching an exponential curve has been obtained in the present work (Fig. 3), although the ambient temperature range was significantly lower than in the aforementioned SEARCH study. No linear or exponential relationship has been found with respect to relative humidity in the present study.

### *3.3. Non-traffic urban ammonia sources*

As is mentioned in some works in the literature (Reche et al., 2015; Pandolfi et al., 2012), sources other than traffic can influence urban ammonia concentrations and they have been investigated in the present

study. For this purpose, a wind direction analysis was performed by taking advantage of the high time resolution provided by the ammonia monitor. Fig. 4 shows a polar plot of 10-min ammonia concentrations and wind data during the measuring period. As can be seen in this figure, the maximum ammonia concentrations (8–10 μg $m^{-3}$) were recorded when wind direction was blowing from an upwind sector between 220°-250° with moderate wind speeds (2–6 m $s^{-1}$). Significantly lower ammonia concentrations were observed during low wind speed conditions from other sectors, suggesting a moderate contribution of the main local source of ammonia, i.e. road traffic, to the levels registered during the sampling period.

These results point to a potential source of ammonia located in the SW sector whose emissions can reach the measurement point by a gentle advection of air masses (moderate wind speed and marked wind direction) at the local scale. The presence of a wastewater treatment plant in this direction with a distance of 1.4 km from the CIEMAT site (Fig. 1) could be responsible for the observed concentrations. Fig. 5 shows wind and $NH_3$ evolution during a specific day of the episode. It can be seen that even for low to moderate wind speeds the ammonia concentrations experience the highest increase and maximum values coincide with a southwesterly wind direction.

Wastewater treatment plants have been identified as having a significant influence on ammonia ambient concentrations in urban areas (Reche et al., 2012, 2015; Upadhyay et al., 2013; Revuelta et al., 2014). Although wastewater treatment plants can present technological differences, the location of these plants requires a river flow for treated water drainage. The metropolitan area of Madrid has eight wastewater treatment plants, six of them within the Madrid city and a half of them located along the Manzanares riverbed. This river flows northwestsoutheast in the most meridional part of the Madrid region and receives the effluents of three wastewater treatment plants that treat the waste water of different districts of the city with a total annual flow of 267 $Mm^{-3}$ of treated water (http://www.madrid.es/portales/munimadrid/es). VIVEROS (the wastewater treatment plant in Fig. 1) is the closest plant to the measurement site of the present study, and it is the third in ranking in terms of treated water flow (28 $Mm^{-3}\,y^{-1}$) of the Madrid region.

In terms of atmospheric emissions, the most important species emitted by wastewater plants in general are greenhouse gases ($CO_2$, $CH_4$ and $N_2O$). However, these are not considered in terms of national emissions inventories, as they are not significant. The same consideration occurs with other pollutants, such as non-methane volatile organic compounds (NMVOCs) and $NH_3$, for which these plants are usually considered of minor and local importance, except for odor issues. For these reasons, worldwide emission estimates for these type of sources are not only scarce in but also the fact of obtaining emission factors is a difficult task, as collection, treatment, and storage systems are very facility-specific and treatment and/or storage operations vary widely among the different plants in size and treatment degree. The most

common technology for treatment in public wastewater plants around the world is the aerobic treatment of activated sludge, where raw waste water is mixed with sludge of living aerobic microorganisms that is activated in a mechanically-aerated tank (US EPA, 1994). Gaseous emissions can occur by diffusive and/or convective mechanisms. These components diffuse or volatilize into the air in an attempt to reach equilibrium between the aqueous and vapor phases. Convection occurs when air flows over the water surface, sweeping volatile vapors from the water surface into the air. The rate of volatilization is directly related to the velocity of the airflow over the water surface. Other factors that can affect that rate are the wastewater surface area, ambient temperature and atmospheric turbulence. Classic handbooks on emission factor estimation and emission inventories (US EPA, 1994, 1995; EEA, 2013) only consider NMVOCs as emitted species in this type of treatment plant. Nevertheless, approximate estimates for $NH_3$ emissions from sewage treatment plants can be found in the literature. For example, Battye et al. (2003) provide an emission factor of 0.15 $gNH_3\ m^{-3}$ treated water. This emission factor leads to an emission rate for the VIVEROS activated sludge treatment plant of roughly at least 28 $KgNH_3\ day^{-1}$. This figure can be considered significant in terms of annual emissions as this specific plant, working on a 24/7 and 365-day basis, would probably exceed the annual limit for ammonia emissions established by the present Spanish normative (10,000 kg $year^{-1}$) (Royal Decree RD 508/2007) for industrial facilities. However, at present, no official emission rates on air pollutants are provided by these installations in the official Spanish emission inventory (PRTR, 2015).

### *3.4. Formation of secondary aerosols*

Secondary aerosols are the result of chemical transformations from gaseous precursors (usually $SO_2$, $NO_x$, $NH_3$, and NMVOCs) that give rise to both secondary inorganic aerosols (SIA) and secondary organic aerosols (SOA). Focusing on SIA, $SO_2$ is the main gaseous precursor in areas with industrial and maritime traffic influence (Pérez et al., 2016a,b), whereas in typical urban areas with low $SO_2$ emission levels such as Madrid $NO_x$ emitted by road traffic is the main source of secondary inorganic aerosol. Ambient concentrations of SIA are very dependent on local source emissions, also being modulated by meteorology and ambient features. However, regional-to long-range transport processes of secondary aerosols are not unusual (Squizzato et al., 2012; Revuelta et al., 2012). This causes a great heterogeneity of ambient concentrations in different areas around the world including Europe (Putaud et al., 2010) and Spain (Querol et al., 2004).

In Madrid, SIA accounts for the 20 and 24% of the $PM_{10}$ and $PM_{2.5}$ mass concentrations, respectively, which are mainly observed in the form of calcium and ammonium sulfate and nitrate (Artíñano et al., 2004). Source apportionment studies (Salvador et al., 2004; Querol et al., 2004) have identified road traffic as the main producer (> 70%) of $NO_3^-$ in the $PM_{10}$ mass, also contributing to a quarter of the total $NH_4^+$. However,

there is a non-specific SIA source that includes a variety of local or regional sources and constitutes the SIA urban background, that contributes to most of the $NH_4^+$ and a half of the $SO_4^{2-}$ mass (Salvador et al., 2004).

In the present study, non-refractory species were measured during the experimental period with an ACSM at the experimental site. On average, the contribution of the sum of the main three inorganic species ($NO_3^-$, $SO_4^{2-}$, $NH_4^+$) to the total $PM_1$ mass was 25% (Fig. 6), being mostly attributed to $NO_3^-$ with 17%. Occasionally, the SIA contribution reached almost 100% of the $PM_1$ mass whereas the maximum contributions of $NO_3^-$, $SO_4^{2-}$ and $NH_4^+$ were 90, 28 and 26%, respectively (hourly values).

The contribution of SIA and the other non-refractory species was highly variable. Like those of gaseous ($NH_3$, $SO_2$, NO, $NO_2$) and particulate ($PM_1$, $PM_{2.5}$ and $PM_{10}$) pollutants their concentrations during the measurement period experienced significant variations (Fig. 7) associated to changes in meteorological conditions and local emission influence.

Meteorological parameters (two-height temperature, relative humidity, wind speed and direction) indicate ventilation (high wind speed) and accumulation (low wind speed and surface temperature inversion) periods that can be clearly identified. The first part of the experimental period (December 16–20) shows the progressive increase of the aerosol components dominated by organic species (high relative contribution, % in Fig. 7) and a decrease during the weekend coinciding with the advection, i.e. light to moderate winds, that diminished the ambient concentrations of gaseous and particulate ($PM_1$, $PM_{2.5}$ and $PM_{10}$) fractions. Nevertheless, the nitrate evolution that also shows an increase during this period exhibits a unique maximum during the afternoon that is associated to the $NH_4^+$ evolution. This daily pattern was also observed during the second part of the episode where ambient PM concentrations, being organic enriched, increased again as did the ammonia concentrations. Nitrate and ammonium show high concentrations, presenting a similar time evolution, whereas the sulfate concentration appears to be of low significant in this case, pointing at ammonium nitrate as the main component of SIA in this period.

Fig. 8 shows the cross-correlation of $NH4^+$ with $SO_4^{2-}$ and $NO_3^-$ in terms of equivalents. It is well known that in the atmosphere NH4+ is preferentially associated with free (non sea salt) $SO_4^{2-}$, such as $(NH_4)_2SO_4$ (Seinfeld and Pandis, 2016). For the period of the present study, most of the $SO_4^{2-}$ and $NH_4$+ values appeared over the 1:1 line (Fig. 8a), revealing an excess of $NH_4$+ with respect to $SO_4^{2-}$ most of the time, which presented very low concentrations. The free $NH_4^+$ was thus associated with other anions. The low concentrations of $Cl^-$ during the period (Fig. 7) and the slope of the linear regression between $NO_3^-$ and $NH_4^+$, being close to unity, strongly suggests that most of the acid nitrate was neutralized by excess $NH_4^+$ to form ammonium nitrate ($NH_4NO_3$) (Fig. 8b). The spatial distribution of both species (Fig. 9) confirms the

exact location of the $NH_3$ source in this study, close to the experimental site. The high volatility of ammonium nitrate particles at relatively high temperatures and low humidity levels prevents this type of SIA from reaching moderately high values in Madrid (Mirante et al., 2014) unless specific conditions are achieved. During this winter period, unusual stagnant atmospheric conditions prevailed for many days favoring the progressive accumulation of $NO_2$ and $NH_3$ emissions from local sources that subsequently reacted to form particulate $NH_4NO_3$ that remained stable due to the low temperatures.

Fig. 10 shows the average daily pattern of the particle number size of distribution (PNSD) with the modal diameter, the relative contribution of the particulate components, gaseous pollutants and meteorology during the measurement period. Bimodal size distributions were observed almost all through the day, suggesting that aerosols of different origin are present in the atmosphere. During daylight hours, a high number of ultrafine particles were detected at the measurement site with a daily maximum between the hours of 9:00–10:00 h (LT) being dominated by Aitken-mode particles with a mainly organic composition (Fig. 10). This is a typical behavior of ultrafine particles at this site, due to the impacts of traffic related emissions in the morning (Gómez-Moreno et al., 2011). Only unimodal aerosol distributions were observed between 12:00–18:00 h (LT) when the concentrations of $NO_3^-$, $NH_4^+$ and $NH_3$ were the highest registered daily, indicating the predominance of aerosols with the same secondary origin (Revuelta et al., 2012).

## 4. Conclusions

Ambient concentrations of $NH_3$ were measured online at an urban background site during one month in the winter of 2014–2015. The mean value was above the previous results that were obtained at urban background sites in Madrid according to other studies. Probably, the meteorological conditions (strong stability and episodic conditions) in this period played an important role in the observed concentrations of the present study. Significant variations of $NH_3$ levels were observed throughout the day, being associated to different sources and processes.

The results of this study are in agreement with other studies and confirm that the location of the sampling point (traffic, suburban, rural) has a strong influence on ammonia concentration levels and on the relative strength of traffic and additional sources.

Unlike other studies that were performed in different geographical and seasonal conditions, in the present study no linear correlation was found between temperature and ammonia concentrations in this winter period, although an exponential fit has been derived. On the other hand, a significant correlation over a short time span between traffic gaseous pollutants and the measured ammonia was not found. The rapid

measurement technique used in this study has also contributed to interpreting increases and variations of ammonia and related particulate species, specifically ammonium nitrate emissions that seem to be the dominant secondary inorganic species in Madrid. Despite the fact that ammonium sulfate is the first documented way to form secondary inorganic aerosol (Seinfeld and Pandis, 2016), it seems that in this case the spatial and temporal coincidence of sources of precursors of $NO_3^-$ and $NH_4^+$ favors the formation of this species. In this sense, the traffic source has not been the driving variable of ammonia variations over a short time span at this urban background site in Madrid. However, other urban sources have been considered.

Taking advantage of the high time resolution obtained for ammonia data, provided by the CELAS technique, an interesting relation of the $NH_3$ short-range variations and wind direction has been observed, which provides evidence of the influence of a specific ammonia source consisting of a wastewater treatment plant located at a distance of 1.4 km from the measurement site of the present study. Maximum hourly values measured for ammonia (8.92 μg $m^{-3}$) were recorded, coinciding with the transport of the air mass from this plant. These emissions have contributed to the formation of secondary inorganic aerosols that were measured at the site that can eventually represent >90% of the total $PM_1$ mass. These results highlight the importance of considering the wastewater treatment plants as ammonia sources in the emission inventories for particulate matter. Improvements of these inventories will contribute to support air quality modeling for accurate secondary particulate formation processes.

## Acknowledgements

This work has been carried out within the framework of the PROACLIM project (CGL2014-52877R) and the FPI pre-doctoral research grant BES-2012-056545 of Marta Becerril Valle grant under the Spanish Ministry of Economy and Competitiveness (MINECO) Research and Innovation Plan. SolMa Environmental Solutions, SLU are especially acknowledged for the instrumental support provided during this experimental study. The authors are also very grateful to the two anonymous reviewers for their helpful comments that have contributed to the improvement of the manuscript.

## Appendix A. Supplementary data

Supplementary data related to this article can be found at http://dx.doi.org/10.1016/j.atmosenv.2018.06.037.

## References

Artíñano, B., Salvador, P., Alonso, D.G., Querol, X., Alastuey, A., 2004. Influence of Traffic on the PM10 and PM2.5 urban aerosol fractions in Madrid (Spain). Sci. Total Environ. 334–335, 111–123.

Ayuntamiento de Madrid, 2016. Plan A: Plan de Calidad del Aire y Cambio Climático de la Ciudad de Madrid. http://www.madrid.es/UnidadesDescentralizadas/ Sostenibilidad/CalidadAire/Ficheros/PlanAireyCC_092017.pdf, Accessed date: 20 December 2017.

Battye, W., Aneja, V.P., Roelle, P.A., 2003. Evaluation and improvement of ammonia emissions inventories. Atmos. Environ. 37, 3873–3883.

Bobbink, R., Hicks, K., Galloway, Spranger, T., Alkemade, R., Ashmore, M., Bustamante, M., Cinderby, S., Davidson, E., Dentener, F., Emmett, B., Erisman, J.-W., Fenn, M., Gilliam, F., Nordin, A., Pardo, L., De Vries, W., 2010. Global assessment of nitrogen deposition effects on terrestrial plant diversity: a synthesis. Ecol. Appl. 20 (1), 30–59.

Biswas, K.F., Ghauri, B.M., Husain, L., 2008. Gaseous and aerosol pollutants during Fog and clear episodes in South Asian urban. Atmos. Environ. 42, 7775–7785.

Carslaw, D.C., Ropkins, K., 2012. Openair—an R package for air quality data analysis. Environ. Model. Software 27–28, 52–61.

Chang, Y., Zou, Z., Deng, C., Huang, K., Collett, J.L., Lin, J., Zhuang, G., 2016. The importance of vehicle emissions as a source of atmospheric ammonia in the megacity of Shanghai. Atmos. Chem. Phys. 16, 3577–3594. http://dx.doi.org/10.5194/acp-163577-2016.

Crenn, V., Sciare, J., Croteau, P.L., Verlhac, S., Fröhlich, R., Belis, C.A., Aas, W., Äijälä, M., Alastuey, A., Artiñano, B., Baisnée, D., Bonnaire, N., Bressi, M., Canagaratna, M., Canonaco, F., Carbone, C., Cavalli, F., Coz, E., Cubison, M.J., Esser-Gietl, J.K., Green, D.C., Gros, V., Heikkinen, L., Herrmann, H., Lunder, C., Minguillón, M.C., Močnik, G., O'Dowd, C.D., Ovadnevaite, J., Petit, J.-E., Petralia, E., Poulain, L., Priestman, M., Riffault, V., Ripoll, A., Sarda-Estève, R., Slowik, J.G., Setyan, A., Wiedensohler, A., Baltensperger, U., Prévôt, A.S.H., Jayne, J.T., Favez, O., 2015. ACTRIS ACSM intercomparison – Part 1: reproducibility of concentration and fragment results from 13 individual Quadrupole Aerosol Chemical Speciation Monitors (Q-ACSM) and consistency with co-located instruments. Atmos. Meas. Tech. 8, 5063–5087. http://dx. doi.org/10.5194/amt-8-5063-2015.

European Environment Agency, 2013. European Union Emission Inventory Report 1990–2010 under the UNECE Convention on Long-range Transboundary Air Pollution (LRTAP).EEA Technical report 8. http://www.eea.europa.eu/ publications/eu-emission-inventory-report-1990-2010.

Gómez-Moreno, F.J., Pujadas, M., Plaza, J., Rodríguez-Maroto, J.J., Martínez Lozano, P., Artíñano, B., 2011. Influence of seasonal factors on the atmospheric particle number concentration and size distribution in Madrid. Atmos. Environ. 45, 3169–3180.

Gómez-Moreno, F.J., Alonso, E., Artíñano, B., Juncal-Bello, V., Iglesias-Samitier, S., Piñeiro Iglesias, M., López Mahía, P., Pérez, N., Pey, J., Ripoll, A., Alastuey, A., de la Morena, B.A., García, M.I., Rodríguez, S., Sorribas, M., Titos, G., Lyamani, H., AladosArboledas, L., Latorre, E., Tritscher, T., Bischof, O.F., 2015. Intercomparisons of mobility size spectrometers and condensation particle counters in the frame of the Spanish atmospheric observational aerosol network. Aerosol. Sci. Technol. 49, 777–785.

Harrison, R., Jones, M., 1995. The chemical composition of airborne particles in the UK atmosphere. Sci. Total Environ. 168, 195–214.

Harrison, R.M., Jones, A.M., Beddows, D.C.S., Derwent, R.G., 2013. The effect of varying primary emissions on the concentrations of inorganic aerosols predicted by the enhanced UK Photochemical Trajectory Model. Atmos. Environ. 69, 211–218.

Heeb, N.V., Saxer, C.J., Forss, A.M., Brühlmann, S., 2008. Trends of no-, NO2-, and NH3 emissions from gasoline-fueled Euro-3- to Euro-4-passenger cars. Atmos. Environ. 42, 2543–2554.

Ianniello, A., Spataro, F., Esposito, G., Allegrini, I., Rantica, E., Ancora, M.P., Hu, M., Zhu, T., 2010. Occurrence of gas phase ammonia in the area of Beijing (China). Atmos. Chem. Phys. 10, 9487–9503.

Link, M.F., Kim, J., Park, G., Lee, T., Park, T., Babar, Z.B., Sung, K., Kim, P., Kang, S., Kim, J.S., Choi, Y., Son, J., Lim, H.J., Farmer, D.K., 2017. Elevated production of $NH_4NO_3$ from photochemical processing of vehicle exhaust: implications for air quality in the Seoul Metropolitan Region. Atmos. Environ. 156, 95–101.

Meng, Z.Y., Lin, W.L.X., Jiang, M., Yan, P., Wang, Y., Zhang, Y.M., Jia, X.F., Yu, X.L., 2011. Characteristics of atmospheric ammonia over Beijing, China. Atmos. Chem. Phys. 11, 6139–6151.

Mirante, F., Salvador, P., Pio, C., Alves, C., Artiñano, B., Caseiro, A., Revuelta, M.A., 2014. Size fractionated aerosol composition at roadside and background environments in the Madrid urban atmosphere. Atmos. Res. 138, 278–292,. http://dx.doi.org/10.1016/j.atmosres.2013.11.024.

Nowak, J.B., Neuman, J.A., Bahreini, R., Middlebrook, A.M., Holloway, J.S., McKeen, S.A., Parrish, D.D., Ryerson, T.B., Trainer, M., 2012. Ammonia sources in the California South Coast Air Basin and their impact on ammonium nitrate formation. Geophys. Res. Lett. 39. http://dx.doi.org/10.1029/2012gl051197. L07804.

Pandolfi, M., Amato, F., Reche, C., Querol, X., Alastuey, A., 2012. Summer ammonia measurements in a densely populated Mediterranean city. Atmos. Chem. Phys. 12, 7557–7575.

Pay, M.T., Jiménez-Guerrero, P., Baldasano, J.M., 2012. Assessing sensitivity regimes of secondary inorganic aerosol formation in Europe with the CALIOPE-EU modeling system. Atmos. Environ. 51, 146–164.

Pérez, N., Pey, J., Reche, C., Cortés, J., Alastuey, A., Querol, X., 2016a. Impact of harbour emissions on ambient PM10 and PM2.5 in Barcelona (Spain): evidences of secondary aerosol formation within the urban area. Sci. Total Environ. 571, 237–250. http://dx. doi.org/10.1016/j.scitotenv.2016.07.025.

Perrino, C., Catrambone, A., Di Menno Di Bucchianico, A., Allegrini, I., 2002. Gaseous ammonia in the urban area of Rome, Italy and its relationship with traffic emissions. Atmos. Environ. 36, 5385–5394.

Putaud, J.P., Van Dingenen, R., Alastuey, A., Bauer, H., Birmili, W., Cyrys, J., Flentje, H., Fuzzi, S., Gehrig, R., Hansson, H.C., Harrison, R.M., Herrmann, H., Hitzenberger, R., Hüglin, C., Jones, A.M., Kasper-Giebl, A., Kiss, G., Kousa, A., Kuhlbusch, T.A.J., Löschau, G., Maenhaut, W., Molnar, A., Moreno, T., Pekkanen, J., Perrino, C., Pitz, M., Puxbaum, H., Querol, X., Rodriguez, S., Salma, I., Schwarz, J., Smolik, J., Schneider, J., Spindler, G., ten Brink, H., Tursic, J., Viana, M., Wiedensohler, A., Raes, F., 2010. A European aerosol phenomenologye3: physical and chemical characteristics of particulate matter from 60 rural, urban, and kerbside sites across Europe. Atmos. Environ. 44, 1308–1320.

Phan, N.T., Kim, K.H., Shon, Z.H., Jeon, E.C., Jung, K., Kim, N.J., 2013. Analysis of ammonia variation in the urban atmosphere. Atmos. Environ. 65, 177–185.

PRTR, 2015. PRTR-españa State Registry of Emissions and Pollutant Sources. October 2015. http://www.prtr-es.es/informes/fichacomplejo.aspx?Id_Complejo=5730.

Pérez, N., Pey, J., Reche, C., Cortés, J., Alastuey, A., Querol, X., 2016b. Impact of harbour emissions on ambient PM10 and PM2.5 in Barcelona (Spain): evidences of secondary aerosol formation within the urban area. Sci. Total Environ. 571, 237–250.

Querol, X., Alastuey, A., Viana, M.M., Rodríguez, S., Artíñano, B., Salvador, P., Santos, S.G.D., Patier, R.F., Ruiz, C.R., Rosa, J.D.L., Sánchez de la Campa, A., Menéndez, M., Gil, J.I., 2004. Speciation and origin of PM10 and PM2.5 in Spain. J. Aerosol Sci. 35, 1151–1172.

Reche, C., Viana, M., Pandolfi, M., Alastuey, A., Moreno, T., Amato, F., Ripoll, A., Querol, X., 2012. Urban NH3 levels and sources in a mediterranean environment. Atmos. Environ. 57, 153–164.

Reche, C., Viana, M., Karanasiou, A., Cusack, M., Alastuey, A., Artíñano, B., Revuelta, M.A., López-Mahía, P., Blanco-Heras, G., Rodríguez, S., Sánchez de la Campa, A.M., Fernández-Camacho, R., González-Castanedo, Y., Mantilla, E., Tang, Y.S., Querol, X., 2015. Urban NH3 levels and sources in six major Spanish cities. Chemosphere 119, 769–777. http://dx.doi.org/10.1016/j.chemosphere.2014.07.097.

Revuelta, M.A., Harrison, R.M., Núñez, L., Gomez-Moreno, F.J., Pujadas, M., Artíñano, B., 2012. Comparison of temporal features of sulphate and nitrate at urban and rural sites in Spain and the UK. Atmos. Environ. 60, 383–391. http://dx.doi.org/10.1016/j. atmosenv.2012.07.004.

Revuelta, M.A., Artíñano, B., Gómez-Moreno, F.J., Viana, M., Reche, C., Querol, X., Fernández, A.J., Mosquera, J.L., Núñez, L., Pujadas, M., Herranz, A., López, B., Molero, F., Bezares, J.C., Coz, E., Palacios, M., Sastre, M., Fernández, J.M., Salvador, P., Aceña, B., 2014. Ammonia levels in different kinds of sampling sites in the central Iberian Peninsula. In: Proceedings of the 2nd Iberian Meeting on Aerosol Science and Technology, RICTA 2014.

Romanini, D., Ventrillard, I., Méjean, G., Morville, J., Kerste, l E., 2014. Introduction to cavity enhanced absorption spectroscopy. In: In: Gagliardi, G., Loock, H.-P. (Eds.), Cavity-enhanced Spectroscopy and Sensing, Springer Series in Optical Sciences, vol 179 © Springer-Verlag Berlin Heidelberg. http://dx.doi.org/10.1007/978-3-64240003-2_1. 2014.

Ryer-Powder, J.E., 1991. Health effects of ammonia. Plant Oper. Progr. 10, 228–232. http://dx.doi.org/10.1002/prsb.720100411.

Salvador, P., Artíñano, B., Alonso, D.G., Querol, X., Alastuey, A., 2004. Identification and characterisation of sources of PM10 in Madrid (Spain) by statistical methods. Atmos. Environ. 38, 435–447.

Salvador, P., 2018. In: Dominick, A., DellaSala, Goldstein, Michael I. (Eds.), Ozone, $SO_x$ and $NO_x$, Particulate Matter, and Urban Air. Encyclopedia of the Anthropocene, ISBN: 978-0-12-813576-1. Vol. 5 “Contaminants”, 7-21.https://doi.org/10.1016/ B978-0-12-809665-9.09975-4.

Seinfeld, J.H., Pandis, S.N., 2016. Atmospheric Chemistry and Physics: from Air Pollution to Climate Change, third ed. John Wiley & Sons, New York.

Squizzato, S., Masio, M., Innocente, E., Pecorari, E., Rampazzo, G., Pavoni, B., 2012. A procedure to assess local and long-range transport contributions to PM2.5 and secondary inorganic aerosol. J. Aerosol Sci. 46, 64–76.

Sun, K., Tao, L., Miller, D.J., Pan, D., Golston, L.M., Zondlo, M.A., Griffin, R.J., Wallace, H.W., Leong, Y.J., Yang, M.Y.M., Zhang, Y., Mauzerall, D.L., Zhu, T., 2016. Vehicle emissions as an important urban ammonia source in the United States and China. Environ. Sci. Technol. http://dx.doi.org/10.1021/acs.est.6b02805. Publication Date (Web): 29 Nov 2016.

Sutton, M.A., Dragosits, U., Tang, Y.S., Fowler, D., 2000. Ammonia emissions from nonagricultural sources in the UK. Atmos. Environ. 34, 855–869. http://dx.doi.org/10.1016/S1352-2310(99)00362-3.

Trebs, I., Meixner, F.X., Slanina, J., Otjes, R., Jongejan, P., Andreae, M.O., 2004. Realtime measurements of ammonia, acidic trace gases and water-soluble inorganic aerosol species at a rural site in the Amazon Basin. Atmos. Chem. Phys. 4, 967–987 2004.

Upadhyay, N., Sun, Q., Allen, J.O., Westerhoff, P., Herckes, P., 2013. Characterization of aerosol emissions from wastewater aeration basins. J. Air Waste Manag. Assoc. 63 (1), 20–26.
http://dx.doi.org/10.1080/10962247.2012.726693.

U.S. EPA, Environmental Protection Agency, 1994. Air Emissions Models for Waste and Wastewater. EPA-453/R-94–9080A.
https://www3.epa.gov/ttnchie1/software/water/air_emission_models_waste_wastewater.pdf.

U.S. EPA Environmental Protection Agency, 1995. AP42 Fifth Edition. Compilation of Air Pollutant Emission Factors, vol. 1 Stationary Point and Area Sources. (Chapter 4), Section 3 Waste Water Collection, Treatment and Storage. http://www3.epa.gov/ ttnchie1/ap42/ch04/final/c4s03.pdf.

Van Breemen, N., Burrough, P.A., Velthorst, E.J., Van Dobben, H.F., De Wit, T., Ridder, T.B., Reijnders, H.F.R., 1982. Soil acidification from atmospheric ammonium sulphate in forest canopy throughfall. Nature 299, 548–550.

552 Wang, S., Nan, J., Shi, C., Fu, Q., Gao, S., Wang, D., Cui, H., Saiz-Lopez, A., Zhou, B., 2015. Atmospheric
553 ammonia and its impacts on regional air quality over the megacity of Shanghai, China. Sci. Rep. 5, 1584.
554 http://dx.doi.org/10.1038/srep15842.
555 Warneck, P., 2000. Chemistry of the Natural Atmosphere, second ed. Academic Press Inc, New York NY.
556 You, Y., Kanawade, V.P., de Gouw, J.A., Guenther, A.B., Madronich, S., Sierra-Hernández, M.R., Lawler, M.,
557 Smith, J.N., Takahama, S., Ruggeri, G., Koss, A., Olson, K., Baumann, K., Weber, R.J., Nenes, A., Guo, H.,
558 Edgerton, E.S., Porcelli, L., Brune, W.H., Goldstein, A.H., Lee, S.-H., 2014. Atmospheric amines and
559 ammonia measured with a chemical ionization mass spectrometer (CIMS). Atmos. Chem. Phys. 14,
560 12181–12194. http://dx.doi.org/10.5194/acp-14-12181-2014.
561

562 **FIGURES**

563


564

565 Fig. 1. Map showing the Madrid location and the CIEMAT experimental site. The position of the nearby Wastewater (WW)
566 treatment plant (upper left square) has been marked.

567

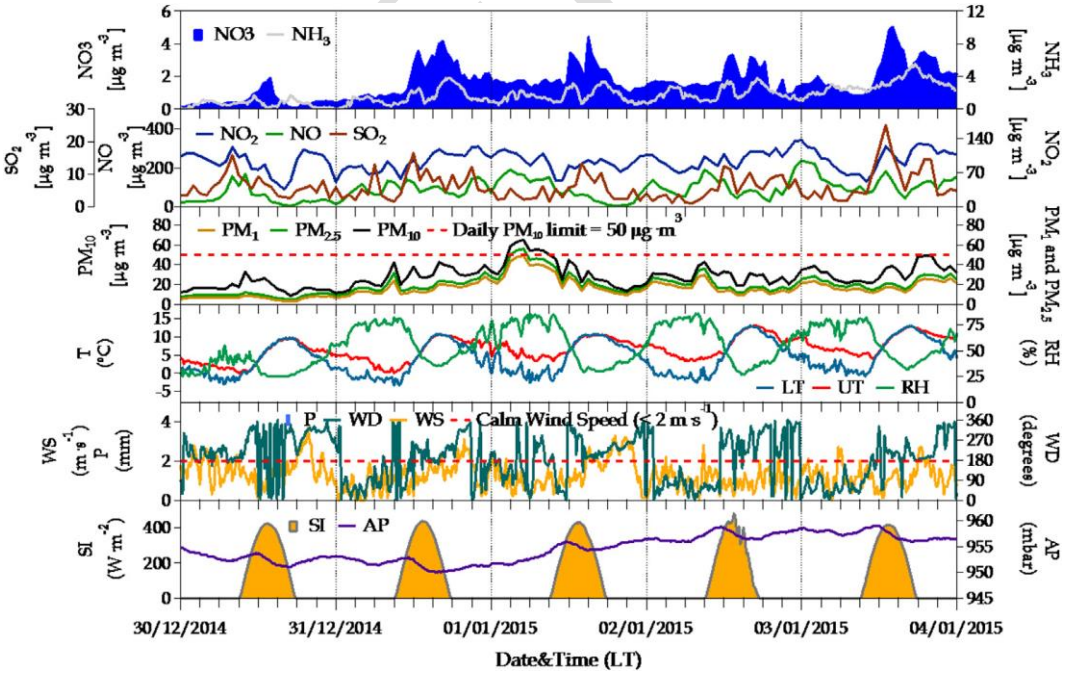


568

569 Fig. 2. Time series of hourly concentrations of some specific aerosol components ($NO_3$ = nitrate), mass concentration
570 of particles at different fractions ($PM_{10}$, $PM_{2.5}$, $PM_1$), gaseous pollutants ($NH_3$, $NO_2$, NO, $SO_2$) and meteorological
571 parameters (LT = lower temperature, UT = upper tem- perature, HR = relative humidity, WS = wind speed, WD = wind
572 direction, P = precipitation, SI = solar irradiance and AP = atmospheric pressure) measured at CIEMAT in the period of
573 December 31, 2014 to January 4, 2015.

574

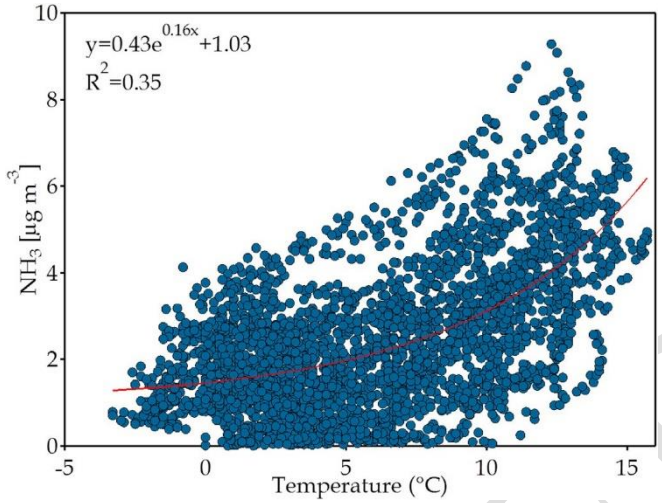


Fig. 3. Ammonia and temperature correlation curve with fitting parameters.

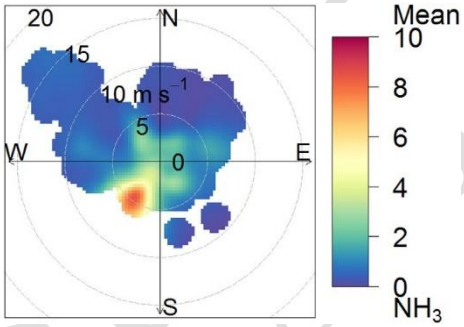


Fig. 4. Polar plot of 10-min averages of $NH_3$ concentrations (μg $m^{-3}$) and wind speed and direction during the measuring period.

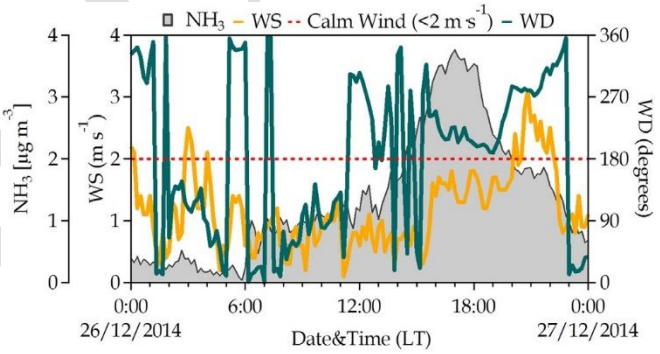


Fig. 5. Ammonia concentrations and wind (WS = wind speed, WD = wind di- rection) series on December 26, 2014.

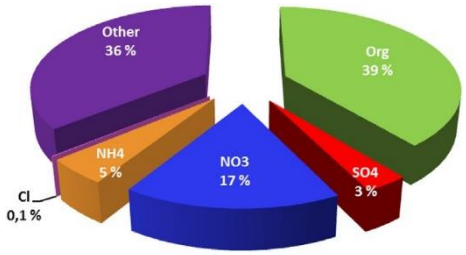


Fig. 6. Average contribution (%) of non-refractory species and other species to the total $PM_1$ mass during the study period.

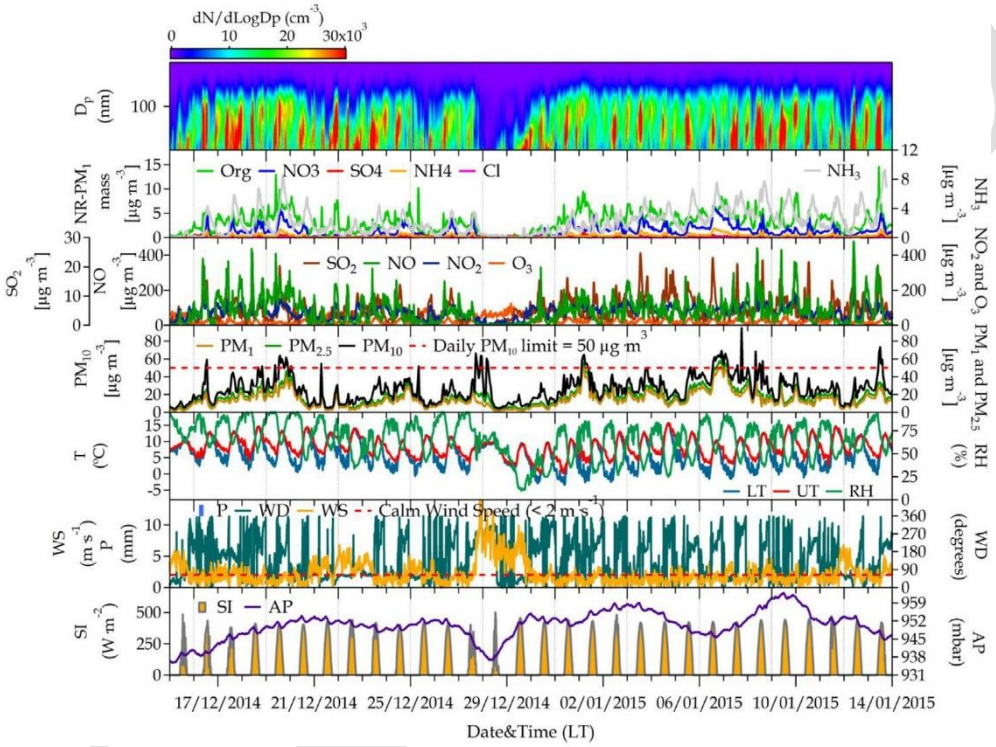


Fig. 7. Time series of 10-min concentrations of: Size distribution (Dp = particle diameter) of total number of particles (N), relative contribution of different species (Org = organic, $NO_3$ = nitrate, $SO_4$ = sulfate, NH4 = ammonium, Cl=Chloride) to the non-refractory $PM_1$ mass, gaseous pollutants ($SO_2$, NO, $NO_2$, $O_3$ and $NH_3$), particulate matter ($PM_{10}$, $PM_{2.5}$ and $PM_1$) concentrations and meteorological vari-ables (LT = lower temperature and UT = upper temperature, HR = relative humidity, WS = wind speed, WD = wind direction, P = precipitation, SI = solar ir radiance and AP = atmospheric pressure), recorded at CIEMAT during the measurement period.

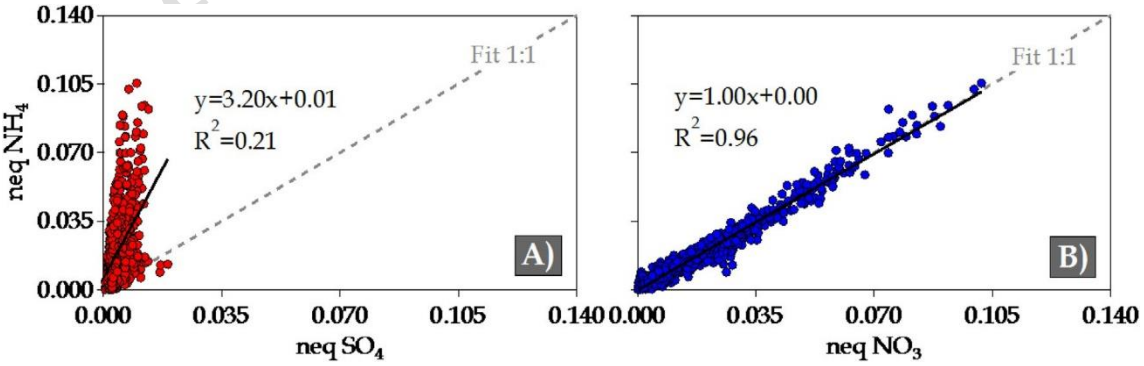

Fig. 8. Linear correlation fit (neq) of: A) ammonium with $SO_4$ and B) ammonium with $NO_3$.

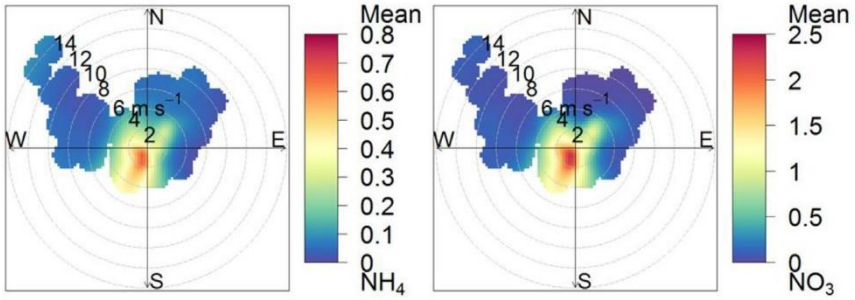


Fig. 9. Polar plots of NH4, (left), $NO3^-$(center) concentrations ($\mu g\ m^{-3}$). Note the different scales used for each figure

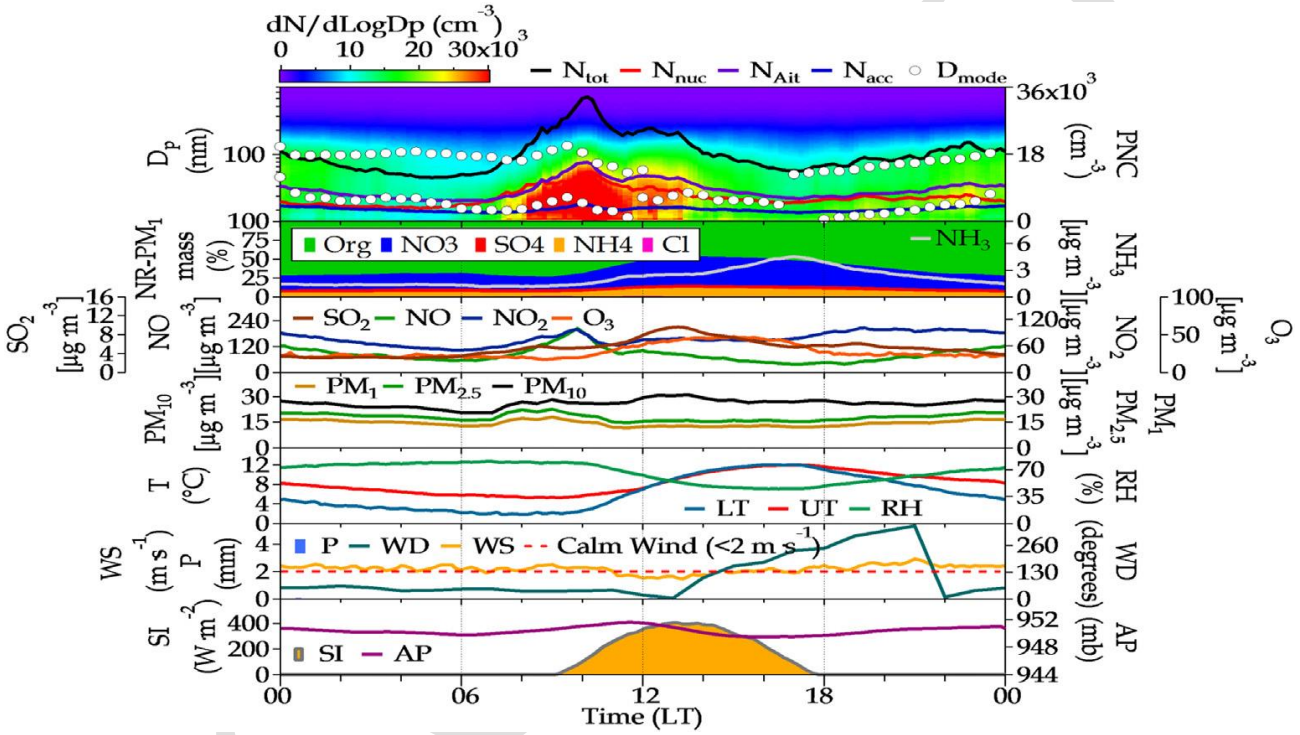


Fig. 10. Average daily pattern of the sizesegregated particle number (Ntot total number of particles, Nnuc nucleation-mode particles, NAit Aitken-mode particles, Nacc accumulation-mode particles), Dmode modal diameter, NR-$PM_1$=percentage of each particulate species (Org=organic, $NO_3$=nitrate, $SO_4$=sulfate,NH4=ammonium, Cl=Chloride) to the sum of non-refractory species measured in $PM_1$, gaseous pollutants ($SO_2$=sulfur dioxide,NH3= ammonia, $NO_2$=nitrogen dioxide, NO= nitrogen oxide, $O_3$ ozone), particulate matter ($PM_{10}$, $PM_{2.5}$ and $PM_1$) and meteorological parameters (LT=Lower, UT= upper temperature, RH=relative humidity, WS=wind speed, WD=wind direction, AP=atmospheric pressure, SI= Solar Irradiance) during the measurement period.

## Appendix A. Supporting material

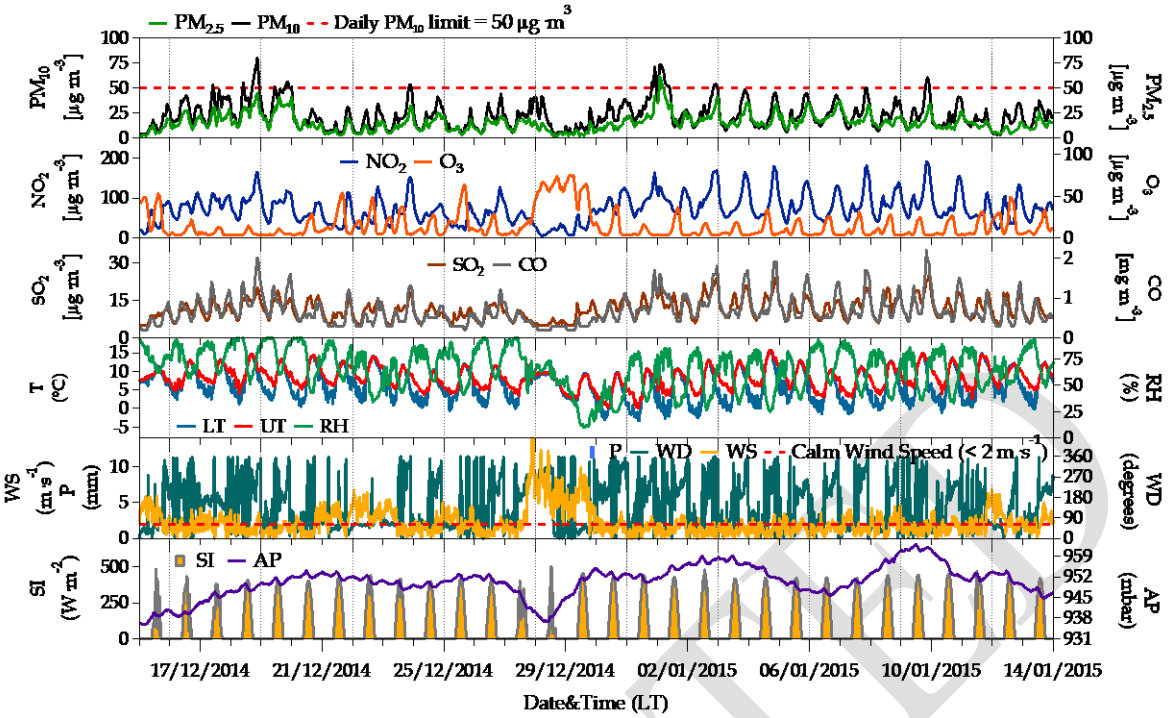


Figure S1. Time series of the hourly concentrations of atmospheric pollutants ($PM_{10}$, $PM_{2.5}$, $NO_2$, $O_3$, $SO_2$, and CO) measured at the Madrid AQMN network (average of 24 stations). Meteorological variables (LT=lower temperature, UT=upper temperature, RH=relative humidity, WS=wind speed, WD=wind direction, P=precipitation, SI=solar irradiance and AP=atmospheric pressure), measured at the CIEMAT experimental site

Table S1. Statistics of hourly values of $NH_3$, $SO_2$, NO, $NO_2$, $O_3$, $PM_1$, $PM_{2.5}$, $PM_{10}$, temperature (T), relative humidity (RH) and wind speed (WS) during the measurement period. Pollutant concentrations are expressed in µg $m^{-3}$, T in ºC, RH in % and WS in m $s^{-1}$.

| Variable | $NH_3$ | $SO_2$ | NO | $NO_2$ | $O_3$ | $PM_1$ | $PM_{2.5}$ | $PM_{10}$ | T | RH | WS |
|---|---|---|---|---|---|---|---|---|---|---|---|
| Minimum | 0.0 | 0.1 | 3.0 | 4.7 | 2.9 | 1.5 | 2.8 | 3.8 | -2.5 | 10.5 | 0.1 |
| Maximum | 8.9 | 25.1 | 412.5 | 198.7 | 93.2 | 52.2 | 61.1 | 94.9 | 15.6 | 95.8 | 13.9 |
| Average | 2.2 | 5.2 | 83.2 | 76.5 | 27.6 | 14.4 | 18.0 | 26.2 | 6.3 | 65.9 | 2.1 |
| Standard Dev. | 1.7 | 3.9 | 70.8 | 33.3 | 18.2 | 9.3 | 10.6 | 14.6 | 4.1 | 18.9 | 1.8 |
| Percentile 90 | 4.7 | 10.3 | 179.2 | 117.7 | 56.5 | 26.2 | 31.4 | 46.3 | 11.9 | 89.3 | 4.3 |

Table S2 Coefficients of determination ($R^2$) of the linear correlation between $NH_3$ and $SO_2$, NO, $NO_2$, $O_3$, $PM_1$, $PM_{2.5}$, $PM_{10}$, temperature (T) and relative humidity (RH).

| $R^2$ | $SO_2$ | NO | $NO_2$ | $O_3$ | $PM_1$ | $PM_{2.5}$ | $PM_{10}$ | T | RH |
|---|---|---|---|---|---|---|---|---|---|
| $NH_3$ | 0.129 | 0.020 | 0.180 | 0.016 | 0.183 | 0.172 | 0.318 | 0.212 | 0.043 |